

The EnMAP hyperspectral imaging spectrometer: instrument concept, calibration and technologies

B. Sang, J. Schubert, S. Kaiser, V. Mogulsky, C. Neumann, K.-P. Förster, S. Hofer, T. Stuffer^a,
H. Kaufmann^b, A. Müller^c, T. Eversberg, C. Chlebek^d

^aKayser-Threde GmbH, Wolfratshauser Str. 48, 81379 Munich, Germany

^bHelmholtz-Zentrum Potsdam Deutsches GeoForschungsZentrum - GFZ, Telegrafenberg A17,
14473 Potsdam, Germany

^cGerman Remote Sensing Center, Münchner Str. 20, 82234 Wessling, Germany

^dGerman Aerospace Center Space Agency, Königswinterer Str. 522-524, 53227 Bonn, Germany

ABSTRACT

The Environmental Mapping and Analysis Program (EnMAP) is a German space based hyperspectral mission planned for launch in 2012. The hyperspectral instrument covers the wavelength range from 420nm to 2450nm using a dual spectrometer layout. Both f/3 spectrometers employ a prism disperser for maximum throughput and are linked to the common foreoptics by a micromechanical field splitter. Together with custom designed silicon and MCT-based detector arrays this sensor design exhibits a peak system SNR of 1000 at 495nm and of more than 300 at 2200nm. Stable and precise in orbit performance is ensured by a multi loop thermal control system and a system calibration which relies on onboard sources as well as a full aperture diffuser.

Keywords: earth observation, remote sensing, hyperspectral imaging, imaging spectrometers, EnMAP

1. INTRODUCTION

Continuous changes in the Earth's environment and the growing impact of anthropogenic factors such as the population increase and fossil resource usage make it necessary to closely monitor the evolution of the terrestrial ecosystem and resources. The large scientific demand for remote sensing data is reflected in multi-mission programs such as ESA's Living Planet and Global Monitoring of Environment and Security (GMES) programs as well as in NASA's Earth Observing System. Data from hyperspectral imagers allow extracting and observing a wide variety of ecosystem parameters from fields such as agriculture, forestry, geology and inland respectively coastal water bodies. To be able to determine these parameters with sufficient precision for model validation it is mandatory to dispose of a stable calibrated sensor system capable of a high signal to noise ratio (SNR). Such sensors allow using advanced processing algorithms e.g. for automated identification and mapping of materials or for spectral unmixing.

Embedded in the GMES program EnMAP is the German response to the need for global hyperspectral coverage. To date there is no sensor in space which is capable of fulfilling all scientific demands. Technology demonstrators such as the HYPERION instrument on EO-1 and CHRIS on Proba have proven the feasibility and the potential of hyperspectral observation from space but are limited with respect to sensor SNR and coverage or spectral range. The EnMAP system which has recently passed the preliminary design review meets the demanding scientific requirements in a fully operational mission scenario. It will provide hyperspectral data with global coverage in an unsurpassed quality. Key performance parameters of the hyperspectral sensor are listed in table 1.

The sun-synchronous orbit with a local time descending node (LTDN) at 11:00 is the optimum choice for good and constant illumination conditions as well as low cloud cover probability. Together with the across track platform pointing capability of $\pm 30^\circ$ the orbit enables global site accessibility within 4 days. At the same time a near repeat track after 4 days permits to revisit a target under similar observation conditions thereby allowing to study the short term evolution of the ecosystem with high precision. Data takes can be acquired with an accumulated length of 5000km along track per day and individual segments ranging from 30km to 1000km. The instrument is a pushbroom type hyperspectral imaging spectrometer with 30km swath width at a ground sampling distance of 30m covering the full range of strong solar irradiation from 420nm to 2450nm. Image data which are recorded at a frame rate of 230Hz are downlinked during

Copyright 2008 Society of Photo-Optical Instrumentation Engineers.

This paper will be published in the SPIE Proceedings Vol. 7086 and is made available as an electronic preprint with permission of SPIE. One print or electronic copy may be made for personal use only. Systematic or multiple reproduction, distribution to multiple locations via electronic or other means, duplication of any material in this paper for a fee or for commercial purposes, or modification of the content of the paper are prohibited.

Table 1 EnMAP mission parameters and instrument capabilities

Parameter	Performance	Parameter	Performance
orbit	sun synchronous “frozen” orbit LTDN 11:00 Inclination 97.9655° 653 km reference altitude	SNR @ 10nm equivalent bandwidth	> 500 @ 495 nm > 150 @ 2200 nm, nadir looking, 30° sun-zenith angle, 0.3 earth albedo
instrument type	push broom hyper spectral imager	smile / keystone	< 20% of a detector element
ground sampling distance / swath	30 m x 30 m, 30 km nadir looking	coregistration	< 20% of a detector element
frame rate	230 Hz nominal (4.3ms integration time)	polarization sensitivity	< 5%
spectral range / broadcast channels	420 nm – 1000 nm (94 channels) 900 nm – 2450 nm (134 channels)	radiometric accuracy / stability	5% absolute, ± 2.5% between calibrations
spectral sampling	6.5 nm average VNIR 10 nm average SWIR	spectral calibration accuracy / stability	< 0.5 nm
MTF	> 25% at 16.6 cyc/km (Nyquist) for all wavelengths across track > 16% at 16.6 cyc/km (Nyquist) for all wavelengths along track	data rate / daily volume (5000 km swath length/day)	866 Mbit/s science data approx. 650 Gbit uncompressed approx. 400 Gbit compressed (512 Gbit of mass memory)

several contacts per day via the Neustrelitz ground station using an X-band link. The maximum image length is limited only by the size of the mass memory and the downlink capacity.

The reference observation situation relevant for the instrument performance has been defined to be nadir looking with a 30° sun-zenith angle illumination, an earth albedo of 30% and a rural aerosol atmosphere with 40km visibility and 2 cm water vapor column. Under these conditions the SNR will be greater than 500 for a 10nm equivalent bandwidth of the spectral channel at 500nm, enabling the most demanding applications such as ocean sensing. In the infrared range an SNR of more than 150 will allow the unique identification of geological materials. Low polarization sensitivity is achieved without the use of polarization scramblers by employing a field splitter approach in combination with a new prism based spectrometer design.

The present paper presents the instrument concept and the optical system as well as highlighting some aspects of the detector technology and the calibration approach.

2. INSTRUMENT CONCEPT

A dual spectrometer approach was chosen to cover the required spectral range from 420nm to 2450nm due to different spectral sampling requirements for the visual near infrared (VNIR) and short wave infrared (SWIR) ranges. A silicon based detector system was selected for the VNIR range from 420nm to 1000nm while the SWIR camera features an MCT diode array which is sensitive from 900nm to 2450nm. For the SWIR spectrometer the spacing of the spectral channels is 10nm on average which is sufficient to resolve the typical mineralogical features around 2 μ m while guaranteeing a good SNR in the range where solar irradiation is low. The spectral sampling interval of the VNIR channel on the other hand has been chosen to be 6.5nm, a compromise between resolving power and keeping the SNR as well as the data volume at acceptable levels. Owing to the demanding polarization sensitivity requirement as well as the high optical throughput necessary to achieve the requested SNR performance the disperser has been chosen to be of prism type. This choice results in an acceptable non-linear dispersion behavior as opposed to the equidistant spectral sampling of a grating based instrument.

The instrument thus features a dual spectrometer concept with individual prism dispersers generating two data sets for VNIR and SWIR channels. For on ground processing frequently these two datasets will be merged to form one hyperspectral data cube for the solar spectrum using the spectral overlap of the two spectrometers from 900nm to 1000nm. The common approach to generate this overlap is to use a single entrance slit combined with a dichroic beam

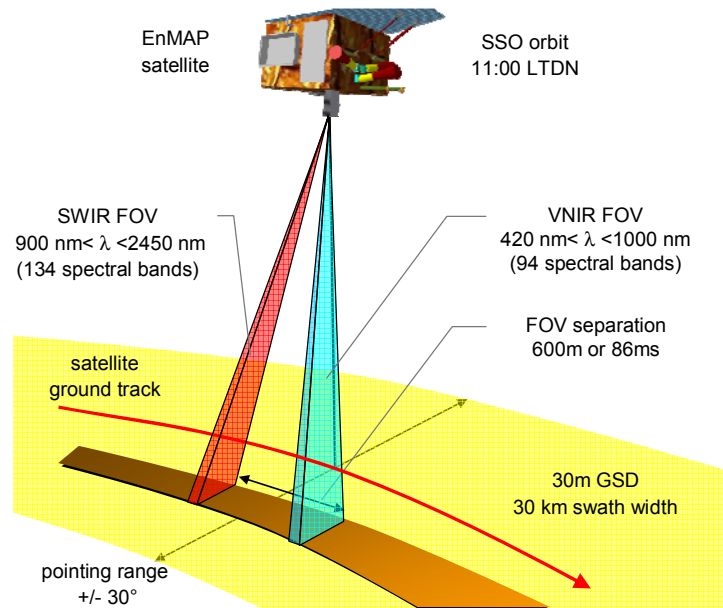


Fig.1 The EnMAP push broom type instrument features a split FOV for VNIR and SWIR spectrometers. Image data for the two channels are recorded with a delay of 86ms. For the chosen orbit and with 30km swath width and $\pm 30^\circ$ off nadir pointing capability global site accessibility is guaranteed within 4 days.

splitter to separate the spectrometer channels. This method allows achieving good coregistration between the spectrometer channels but is problematic with respect to the polarization sensitivity and will result in reduced SNR in the overlap region. EnMAP uses a dual aperture split field of view (FOV) concept to overcome these difficulties. The two spectrometers are coupled to a common telescope via a field splitting unit which features two closely spaced entrance slit apertures and a beam separating optic. Thus both spectrometers deliver full SNR performance in the region of spectral overlap thereby permitting to merge the datasets with high precision and without the drawbacks of increased dichroic induced polarization sensitivity.

The split FOV results in different lines of sight for both spectrometers as illustrated in figure 1. The VNIR FOV travels ahead of the SWIR FOV along the satellite flight direction by 20x the instantaneous field of view (IFOV = $45 \mu\text{rad}$) or approx. 600m on ground. The SWIR data for identical ground target locations is thus recorded with a time delay of 20 frames or 86ms compared to the VNIR data. In order to meet the coregistration requirement the satellite platform must be stable with respect to its line of sight pointing to better than 0.2 IFOV or $9 \mu\text{rad}$ in 86ms.

Several on board facilities for instrument calibration allow consistently monitoring the instrument response and thus enable to achieve a high data quality and reliability after on ground processing. We have foreseen the possibility to calibrate the spectral behavior and the relative radiometric as well as the absolute radiometric properties by means of calibration light sources and a full aperture sun diffuser.

The platform of the EnMAP satellite is a reuse of an existing design with space heritage by OHB-System AG. It features three axis stabilization, an altitude and orbit control system and a mass memory for science data storage. The input image data stream of 866Mbit/s is stored in 5 memory banks composed of SDRAM which are configured such that graceful degradation is tolerated resulting in 512Gbit end of life memory capacity. Lossless data compression is performed offline during data take intervals. The mass memory output is routed through a CCSDS coding unit directly to the 320Mbit/s X-band downlink system.

The EnMAP satellite configuration with the instrument cover structure (ICS) removed is shown in figure 2. The instrument is located on top of the platform compartment in its own section, thereby allowing for easy thermal decoupling from the platform. The instrument optical unit (IOU), which contains the optical system, is suspended on the platform structure by thermally isolating isostatic mounts, while electronics, instrument baffles and radiators are

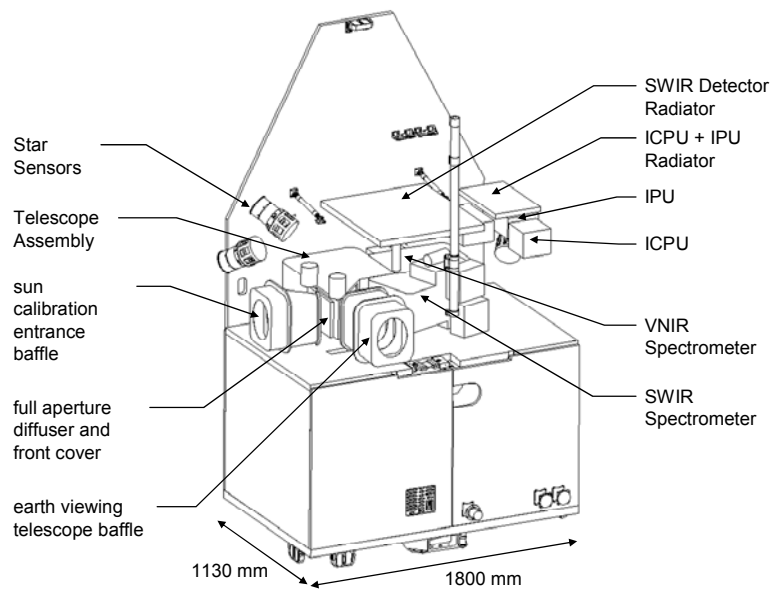


Fig.2 Configuration of the EnMAP satellite with the preliminary design of the instrument optical unit on top of the bus compartment. The protective cover surrounding the instrument which is used as a structural support for the thermal radiators, the instrument electronics and the telescope baffles has been omitted in this view.

mounted to the ICS. Two separate optical entrance apertures including baffles allow for earth observation and sun calibration respectively. The instrument power unit (IPU) which controls the power supply for all instrument subunits and the instrument control and processing unit (ICPU) which performs all control tasks and preprocesses the science data for mass memory storage are implemented fully redundant. While there is only one VNIR focal plane assembly, the SWIR camera system including its cooler and the electronics is featured twice for full redundancy. The design shown in figure 2 is preliminary and will be refined in phase C.

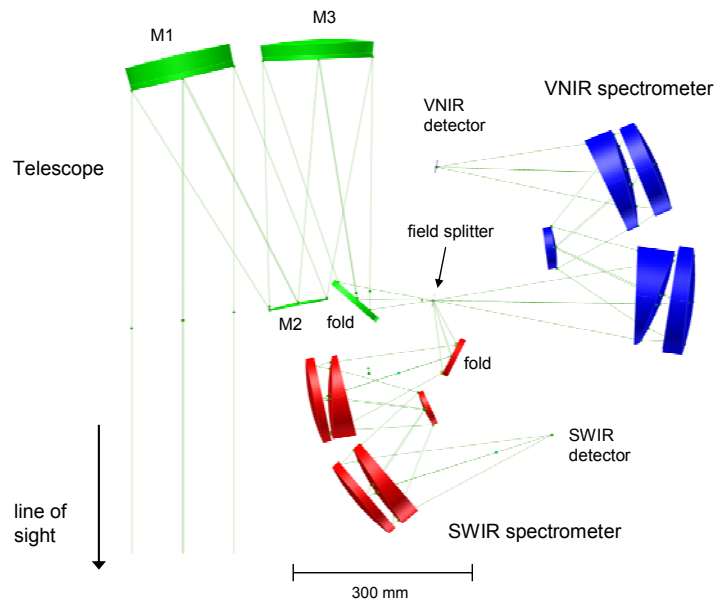


Fig. 3 Layout of the optical system for the EnMAP hyper-spectral instrument.

3. OPTICAL SYSTEM

The optical system of the hyperspectral instrument features a three mirror anastigmat (TMA) telescope which focuses upwelling radiation from earth via a fold mirror onto the field splitter unit (see figure 3). Light transmitted through the dual spectrometer entrance slits contained within the field splitter is directed into the unit magnification spectrometers, which form spectrally resolved images of the slits on the detectors. The optical speed of the system, which is free of artificial vignetting, is $f/3$. The system aperture stop is located at the second telescope mirror generating a telecentric imaging situation at the field stop and thus matching the entrance pupil location of the spectrometers. With a lateral extension of 24mm the detectors define the field for the spectrometers and the telescope. The arrangement of the telescope and the spectrometers is such that all optical elements are located in one plane. It was optimized for minimum volume and a minimum number of reflections as well as for accessibility during integration and ease of alignment.

3.1 Spectrometers

Imaging spectrometer designs for hyperspectral applications must meet very demanding requirements with respect to distortion and image quality. The design forms which are known to be capable of the required performance are the concentric Offner and Dyson types utilizing a grating disperser [1]. For prism based dispersion elements the classical spectrometer design with a collimator – prism – imager configuration [2] or an alternative approach using curved prisms in a non-collimated beam as initially suggested by Féry [3] are possible. For EnMAP we suggest a novel design which uses the very good imaging heritage of an Offner design and combines it with a curved prism disperser. Figure 4 shows the layout of the new design. Following the symmetry of the Offner design two prisms are introduced into an Offner relay, both of which are used in a double pass configuration for increased dispersive power. Initially the prisms are set up similar to the principles described by Féry keeping the angles of incidence constant across the pupil for the central field point. From this starting point the optimization leads to a design that inherits the low distortion properties of the Offner and exhibits good imaging performance in a compact design with minimum volume and all spherical surfaces.

A prism based spectrometer inherently suffers from geometrical distortion along the spectral axis (non-linear dispersion) caused by the nonlinearity of the change in refractive index with wavelength. The spectral sampling distance (SSD) which denotes the difference in central wavelength for neighboring channels is not constant over the spectrum as in a grating spectrometer. The problem can be alleviated by combining different prism materials leading to less SSD variation at the cost of an increased system complexity.

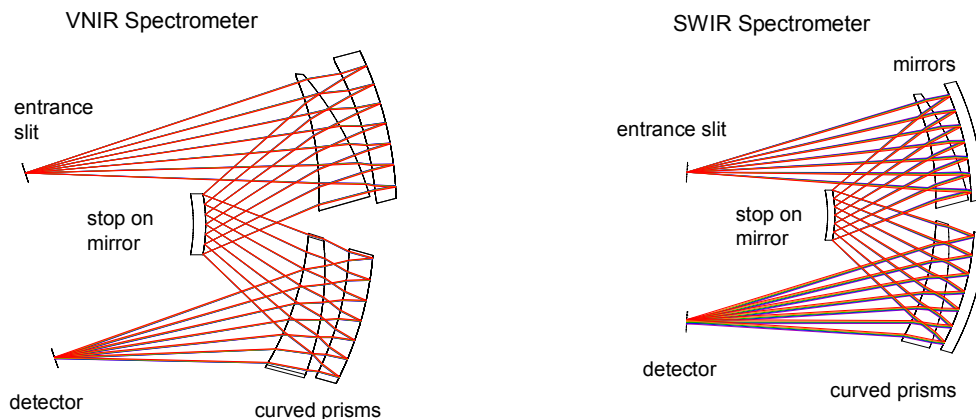


Fig. 4 Both spectrometers VNIR (left) and SWIR (right) employ curved prisms as dispersion and image forming elements. The designs are based on unit magnification Offner relays with a stop on the central mirror. Both plots are to the same scale.

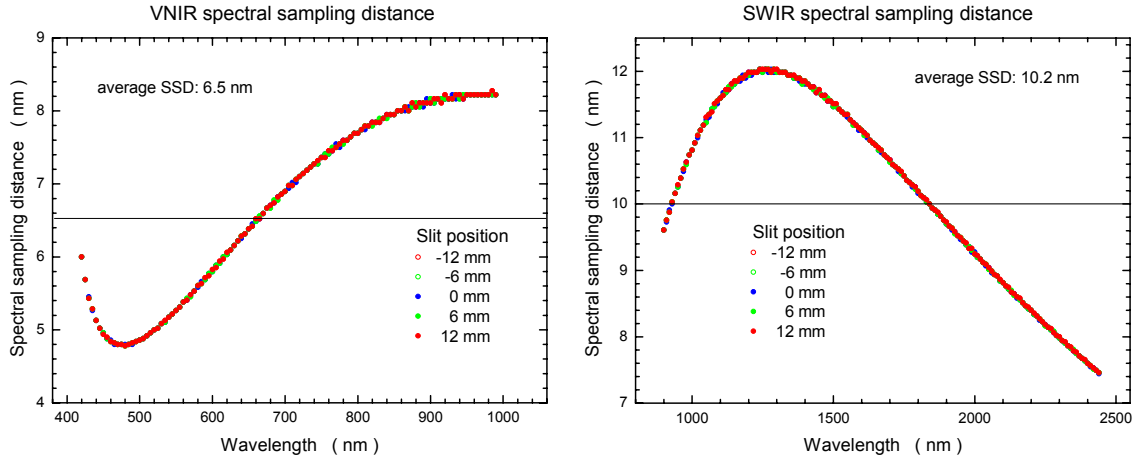


Fig. 5 Spectral sampling distances for the VNIR (left) and SWIR spectral channels (right) as a function of wavelength. The curves depict the difference in center wavelengths for adjoining spectral channels. The non linear behavior is due to the dispersion characteristics of the glasses used for the prisms and their combination.

For the EnMAP SWIR spectrometer a fused silica disperser was chosen based on the dispersion characteristics and the good properties of this material with respect to the space radiation environment. The optical layout of the SWIR spectrometer is shown in figure 4. The dispersive behavior of the system results in an average SSD of 10.2nm with variations of +20% and -25% over the wavelength range and no variation with field position as illustrated in figure 5 which depicts the SSD for all 155 SWIR bands (only 134 of these are transmitted). For the VNIR spectrometer the strong dispersion of glasses in the UV range of the spectrum dictates the use of two compensating glass types. We have selected a combination of fused silica and a flint glass based on the high transmission, good dispersion compensation and relative radiation insensitivity of the materials. Air spacing the prisms avoids problems with CTE mismatch and cementing. With the double element disperser the VNIR spectrometer has a sufficient number of degrees of freedom (DOF) for aberration control even when the internal reflection off the back side of the outer flint prism is used to establish the Offner configuration instead of an additional mirror (see figure 4). For this spectrometer the SSD varies from 4.8nm to 8.2nm with an average of 6.5nm over the full spectral range (see figure 5). For both spectrometers the spectral resolution of a

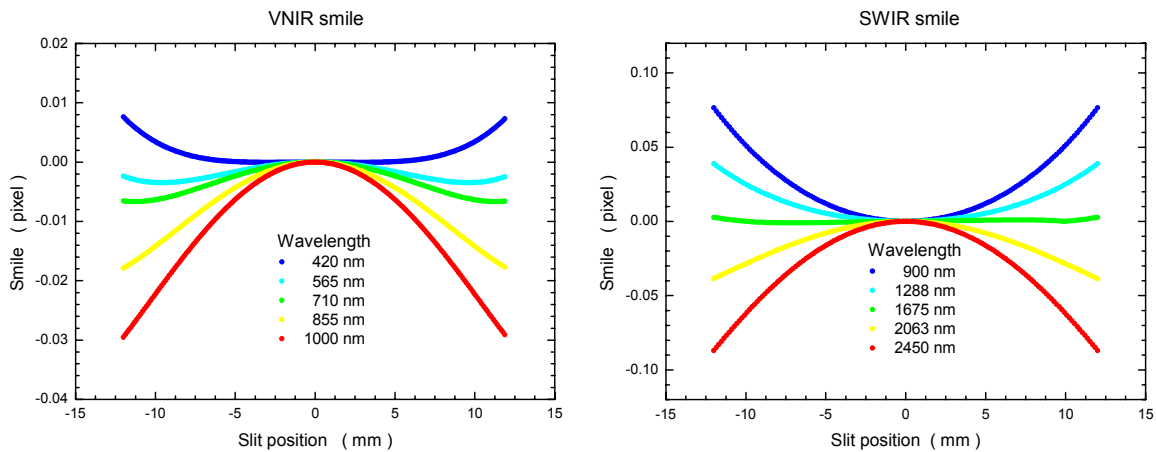


Fig. 6 Smile for both VNIR (left) and SWIR spectrometers (right) as a function of field position in units of spectral pixel size for several wavelengths (spectral pixel pitch is $24\mu\text{m}$ for VNIR and $32\mu\text{m}$ for SWIR). The maximum deviation of the ideal image location in spectral direction is less than $1\mu\text{m}$ in the VNIR and less than $3\mu\text{m}$ for the SWIR at the edges of the field.

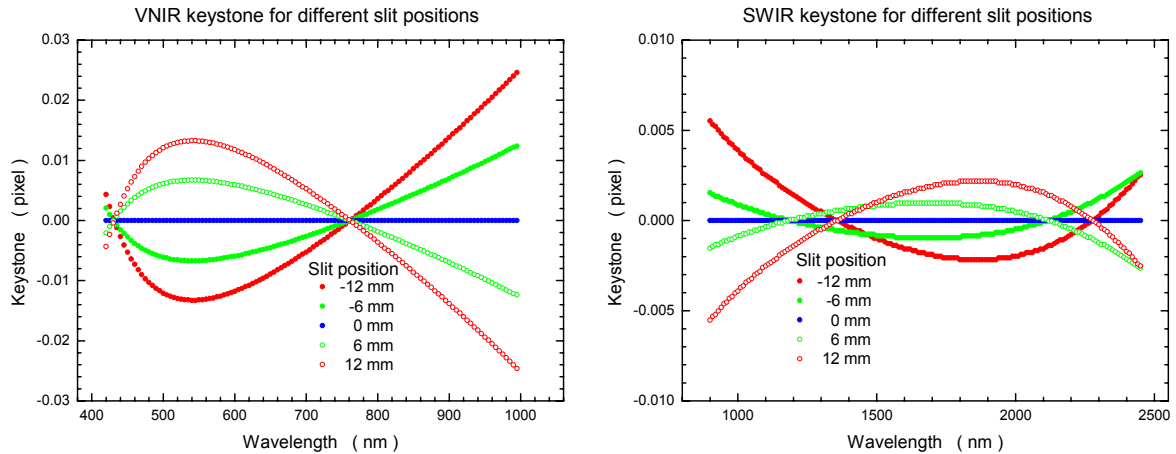


Fig. 7 Keystone distortion for VNIR (left) and (SWIR) spectrometers as a function of wavelength for different across track locations inside the FOV. The distortion is shown in units of pixels ($24\mu\text{m}$ pitch) in across track direction and represents the change in magnification with wavelength.

channel as defined by the FWHM of the corresponding spectral response function (slit function) is similar to the local SSD deviating from this value by less than 10%. This is due to the fact that the spectrometers have been designed with a slightly negative anamorphic imaging behavior. The designs have been filed for patent protection.

The superior performance of the concentric design forms as compared to classical spectrometers is most evident with respect to the geometrical smile and keystone distortions. Figure 6 shows the smile performance for both spectrometers. The plots show the deviation of the slit image from the ideal straight line in units of the spectral pixel pitch for several wavelengths in each range. For the VNIR the center wavelength of any spectral band varies by less than 3% of the local SSD with field position illustrating the very good performance as compared to the allowed 20% deviation. For the SWIR channel the maximum deviation is 9% of the local SSD or 0.77nm for 900nm . The higher value compared to the VNIR is due to the reduced size and smaller number of DOFs of the optical system. Figure 7 depicts the keystone error for the instrument by plotting the deviation of the real image location from the ideal image location along the slit direction as a function of wavelength in units of the spatial pixel pitch. This is equivalent to the variation of the spectrometer magnification with wavelength. For both spectrometers the keystone error is extremely low with a maximum of 2.5% of a pixel for the VNIR and 0.6% for the SWIR, compared with the specification of 20%.

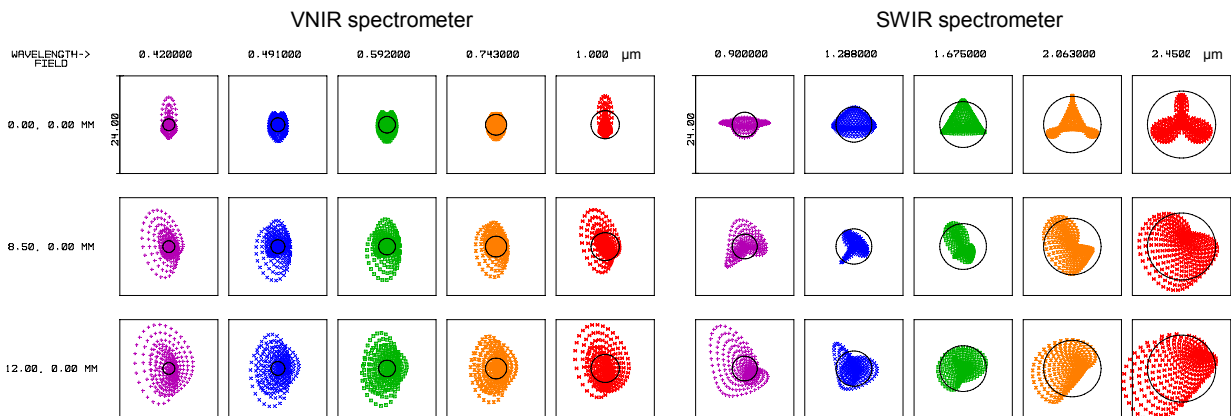


Fig. 8 Spot diagrams for the VNIR spectrometer (left) and the SWIR spectrometer (right). Spots are shown for the center of the slit (top), 70% field (center) and full field bottom for increasing wavelengths (left to right). The size of the reference boxes is $24\mu\text{m}$ and matches the size of the pixel for the VNIR channel. For the SWIR channel the pixel size in spectral direction is $32\mu\text{m}$. The airy disc diameter for the individual wavelengths is indicated by the circles.

The imaging quality of the spectrometers is illustrated by the spot diagrams shown in figure 8 for three field positions and 5 wavelengths in each range together with reference boxes that match the spatial pixel pitch of $24\mu\text{m}$ and circles indicating the airy disc diameter. The good aberration control for the VNIR is demonstrated by the well formed spot distributions with very little variation over wavelength and low acceptable field dependence. The latter is dictated by the size of the spectrometer and reflects the compromise between MTF performance and volume. Spot diameters range from $3.8\mu\text{m}_{\text{rms}}$ for the central field to $8.8\mu\text{m}_{\text{rms}}$ at full field. Due to the smaller size and the single material disperser the SWIR channel shows stronger wavelength dependencies and a somewhat lower performance with spot diameter ranging from $4.4\mu\text{m}_{\text{rms}}$ to $14.2\mu\text{m}_{\text{rms}}$. The MTF of the spectrometers is compliant to the system MTF budget but the SWIR performance will be slightly optimized in Phase C by allowing a slight increase in spectrometer size. A preliminary ghost analysis shows the designs to be uncritical if the back surface of the field splitter is blackened.

Several suppliers have confirmed the manufacturability of the prism elements which will be coated with multilayer low reflectivity AR coatings. The mirrors are made of aluminum using the same mirror technology as for the telescope. They are coated with an enhanced silver coating for the VNIR and with sputtered gold for the SWIR range.

3.2 Telescope

The telescope design is a standard off axis unobscured TMA without intermediate focus locations first introduced by Wetherell and Womble [4]. Similar designs have been used in multiple earth observing missions. The focal length is 522mm with an across track FOV of $\pm 1.31^\circ$. Two mirrors are conics with a 4th order aspherical term while the primary has a regular conic shape. Figure 9 shows the layout of the telescope together with the optical path difference (OPD) for 3 field points. For the shortest wavelength the OPD stays below a quarter of a wave demonstrating the high degree of aberration control which has been achieved. Thus by design, the telescope is diffraction limited for the full spectral range.

The lightweighted mirrors and structure of the telescope are made of aluminum. After single point diamond turning a Nickel-Phosphor (NiP) coating is applied to the mirrors to allow polishing the optical surface. Finally an ion beam figuring process brings the surface form figure down to less than 140nm_{PV} (15nm_{rms}) while retaining the micro roughness of less than 1nm_{rms} from the polishing process. The mirrors are coated with an enhanced silver process in order to maximize the system throughput at 420nm while retaining very good transmission for the full spectral range.

3.3 Field Splitter

The field splitting unit is the central element of the optical system defining the FOV of the telescope as well as for the spectrometers. It serves a dual-purpose by defining the entrance slits for both spectrometers and redirecting the beams

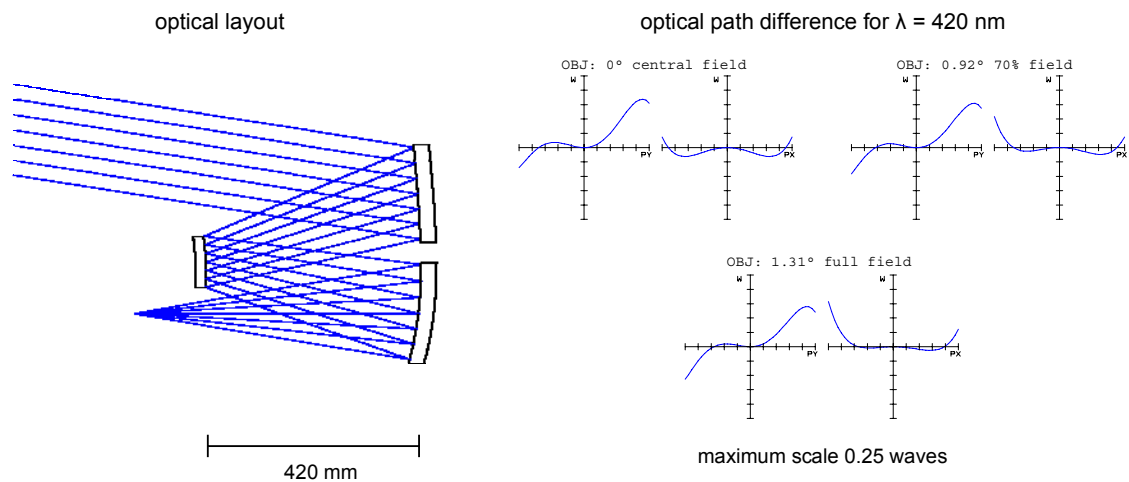


Fig. 9 Optical layout of the Three-Mirror-Anastigmat telescope (left) with a focal length of 522 mm . The optical path difference is less than a quarter wave for a wavelength of 420 nm (right) denoting diffraction limited performance.

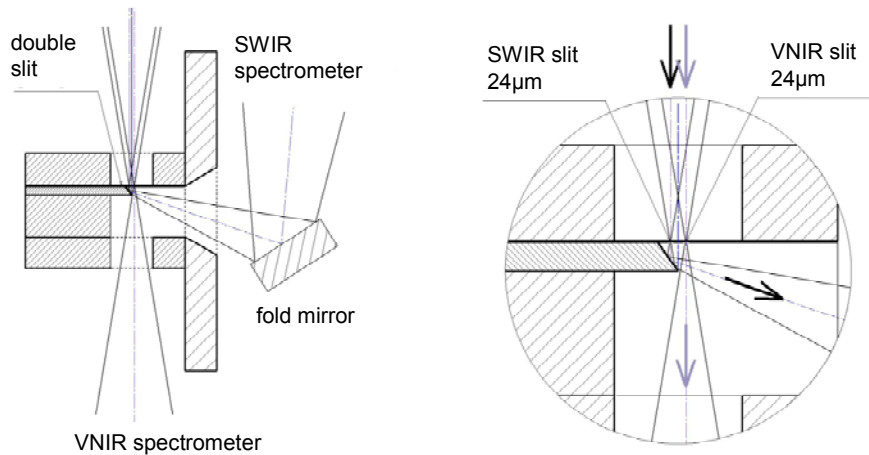


Fig. 10 Principle of the field splitter unit. Light from the telescope enters the unit from the top. After passing through two 24µm wide slits which are separated by 480µm, the radiation for the SWIR spectrometer is redirected by a gold coated micro mirror to achieve beam separation (see detail). The VNIR channel is passed to the spectrometer without further reflection.

into the respective units. A transmissive aperture design for the slits is necessary to separate the telescope compartment from the spectrometers for good straylight control. Figure 10 presents the principle design of the field splitter unit which has been filed for patent. Light from the telescope passes an element which defines the two slit apertures and a micro mirror subsequently reflects the beam associated with the SWIR range before the two beams merge again. To avoid problems with the environmental stability of a protected silver coating on a micro mirror the accommodation of the instrument has been chosen such that the VNIR beam is not subject to a reflection. The distance between the two 24µm wide and 24mm long slits for the split FOV concept must be kept as small as possible in order to keep the separation between the spectrometer FOVs as low as possible for good data coregistration. Technological constraints limit the minimum separation to 480µm because the micro mirror becomes increasingly fragile to manufacture and coat. In addition the suggested slit geometry creates a central self supporting beam between the two apertures. The stiffness of this large aspect ratio beam must be made sufficiently high to endure launch loads as well as to ensure the correct aperture geometry. Very tight tolerances for the slit geometry on the order of 1 µm for width, parallelism and straightness and 0.2µm for edge radii are necessary for good instrument performance.

Silicon wafer based MEMS technology was selected for the aperture forming element since it is known to be capable of the required tolerances routinely due to a large number of well established manufacturing processes. Linked to the choice of material for the slit element the micro mirror is ideally also made of silicon or a CTE matched material such as borosilicate glass. For the mirror critical issues are the aspect ratio of the optical surface, the micro roughness and the mirror coating.

The technological challenges of the field splitter unit were addressed by a bread board study in phase B of the EnMAP program with the aim of testing the manufacturing processes and the alignment of the critical parts. Several wafers were processed to generate the slit geometry as illustrated in figure 11. The complex geometry is necessary to make the central beam stiff enough while allowing the f/3 optical beam to pass unvignetted. Optical opaqueness ($OD > 5$ for all wavelengths) is created by applying a thin layer of aluminum. A nanostructured optically absorbing coating retaining the slit geometry was applied to the side of the wafer which is oriented towards the spectrometer (see inset in figure 11). The geometry of the slit apertures was measured using an automated video measurement system and a scanning electron microscope confirming the required tolerances. Micro mirrors were manufactured from borosilicate glass and from silicon. The surface form was measured to be $< 50\text{nm}_{\text{PV}}$ over the full aperture and $< 25\text{nm}_{\text{PV}}$ within any footprint associated with a single field point. The micro roughness varied from $< 0.3\text{nm}_{\text{rms}}$ for silicon to $< 0.7\text{nm}_{\text{rms}}$ for the glass. Due to problems with the coating of the micro mirrors the design of the field splitter was changed compared to the bread board design so that now only the SWIR channel will be reflected from a micro mirror which will be gold coated.

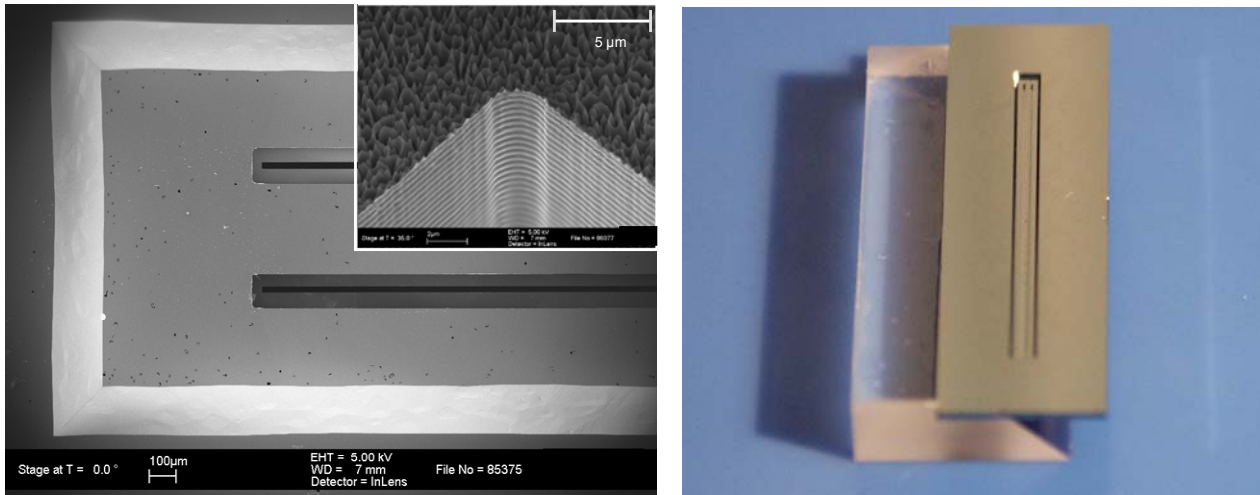


Fig. 11 Results of a bread board study of the field splitter unit. The left hand image shows a scanning electron microscope image of a part of the slit wafer. The back side of the wafer is coated with a micro structured absorbing layer as illustrated by the magnified image of the slit corner in the inset. A demonstrator model which incorporates two redirecting micro mirrors and a dual slit chip aligned and mounted to the necessary precision is depicted at right.

The assembly and alignment was performed using an active optical alignment process. A low outgassing adhesive is used to attach the slit wafer to the micro mirror with an angular alignment tolerance of 1 arcmin and 10µm position tolerance.

4. DETECTORS

In space based hyperspectral imagers of the pushbroom type the focal plane technology is extremely demanding pushing to the limits of the available detector technology. High frame rate area sensors generate up to 60 Mpix/s which must subsequently be digitized with low noise and high dynamic range. Electronic integration time control is necessary to be able to make optimum use of the available light and the pixel full well capacity which is at the limits of the sensor technology due to the high SNR requirements for EnMAP.

4.1 Visual near infrared channel detector

For the silicon based VNIR focal plane array two alternative detector technologies, CMOS and CCD, were studied. The CCD solution involves a frame transfer sensor from e2V which does not allow for direct electronic shuttering. Because of the high frame rate in EnMAP the frame transfer time is always a significant part of the integration time with the result that spectral smear must be removed by post processing. This processing step is known to have a detrimental effect on the data quality by reducing the SNR depending on the spectral signature of the recorded data [5]. Thus, despite the fact that both solutions fulfill the EnMAP requirements, the preferred solution for the VNIR detector is a back thinned, highly integrated CMOS imaging sensor by Fairchild Imaging. Key parameters of the sensor are listed in table 2. The detector will integrate a pinned photodiode with a 5 transistor pixel architecture to allow global electronic shuttering in a stare while scan read out mode. For a pixel pitch of 24µm by 24µm the linear full well capacity is 1 Me⁻ with 2% non-linearity. Using on ground post processing the linearity of the sensor data will be corrected to 0.2% by implementing a polynomial or piecewise linear algorithm with individual correction coefficients for each pixel.

The analog to digital conversion is performed on chip by single slope converters for each column. In order to achieve the high dynamic range and the low noise floor necessary for the EnMAP system performance a dual gain ADC structure will be employed. The pixel voltage output will be amplified using two different gains before being converted in parallel by two 13-bit ADCs. Logic in the front end electronics (FEE) will take the decision on which signal to transmit based on the saturation level of the digital outputs, adding an extra bit to the data stream which encodes the gain selection for post processing. To achieve the required low read noise the chip will output two images for every frame. The first image representing the pixel reset values is stored in the FEE. During the readout of the second image which contains the signal

Table 2 Properties of the baseline EnMAP detectors

	VNIR	SWIR
detector type	Silicon CMOS imaging sensor	MCT + ROIC
readout circuit	pixel based source follower with floating diffusion, dual 13-bit column ADCs with overlapping gain ranges	dual conversion gain CTIA, 8 multiplexed analog outputs
readout mode	stare-while-scan incl. non-destructive readout option integration time control	stare-while-scan integration time control
integration time control	global electronic shutter, 0 to 4.3ms by external control	
spectral range	420 nm – 1000 nm	900 nm – 2450 nm
external quantum efficiency	> 80% at 650 nm (2-layer AR)	> 60% over full spectral range
operational temperature	294 K ± 0.2 K	150 K ± 25 mK
pixel geometry / array format	24 μm(H) x 24 μm(V) 1024(H) x 146(V) active pixels	24 μm(H) x 32 μm(V) 1024(H) x 256(V)
linear full well capacity	1 Me ⁻	low gain 1.2 Me ⁻ high gain 300 ke ⁻
system read noise	low gain 200 e ⁻ _{rms} high gain 50 e ⁻ _{rms} including digital CDS	low gain 290 e ⁻ _{rms} high gain 140 e ⁻ _{rms}
non-linearity	< 2% raw sensor data < 0.2% after digital correction (individual pixel)	

information a hard coded algorithm performs a digital correlated double sampling (CDS) to eliminate the reset noise (kTC noise) by subtracting the corresponding reset value from the signal.

Due to the short integration time the dark current contribution to the signal is small and the detector can be operated at 294K. For thermal stabilization a Peltier element is foreseen to retain the calibration of the sensor throughout the operation.

4.2 Short wave infrared detector

For the SWIR channel a mercury cadmium telluride (MCT) based detector from AIM with a constant external quantum efficiency above 60% was selected. An MCT photodiode array is indium bump bonded to a readout integrated circuit (ROIC) which features a charge transimpedance amplifier (CTIA) per pixel with dual capacities for charge to voltage conversion and a sample capacity for stare while scan operation. The ROIC has 8 analog outputs with a maximum pixel update rate of 10 MHz each and a register based state machine controlling the chip operation as well as the integration time. Key properties of the SWIR detection system are listed in table 2.

A rectangular pixel pitch of 24μm in spatial by 32μm in spectral direction creates sufficient chip area for the pixel circuitry. The integration capacity of the CTIA can be chosen between low and high conversion gain for each spectral row individually. The ratio of the capacitances is designed such that the dynamic requirements of EnMAP are met together with external 14-bit ADCs. This dual gain structure is necessary to cover the inherent high dynamics of the solar flux in the SWIR which changes by 1.5 orders of magnitude from 900nm to 2450nm. Owing to the pixel architecture CDS is not possible with the result of a marginally increased read noise compared to the VNIR channel. The intrinsic linearity of the detector is better than 2% enabling post processing to less than 0.2% on ground.

The small band gap of the MCT which is tailored to deliver a cutoff at a wavelength of 2.5μm makes it mandatory to cool the detector to 150K in operation for dark current suppression. An extremely compact integrated detector cooler assembly was developed by AIM housing the detector array, the ROIC, a pulse tube cooler and a cold shield for background signal reduction in a dewar with an optical window (see figure 12). The pulse tube which uses helium as a working medium is driven by a symmetric flexure bearing compressor. Two pistons move anti-collinear in order to minimize the vibration output of the unit. Using a moving magnet concept and low outgassing materials the cooler is

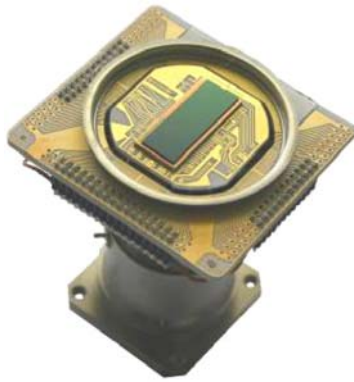


Fig. 12 Components of the SWIR camera system. The integrated detector cooler assembly (left) houses the MCT photodiode array, the ROIC and the pulse tube cooler in a compact dewar. For the picture the top part of the dewar including the cold shield and the optical interface were omitted. The cooling system (right) is composed of a pulse tube cooler driven by a symmetric compressor for low residual vibration output. Pictures courtesy of AIM [6].

designed to have a mean time to failure of more than 60000h. Currently lifetime tests are being performed to confirm this goal. The dissipation of the cooling system for a total heat input at the cold tip of 1W and a heat sink temperature of 294K is less than 30W.

5. SYSTEM PERFORMANCE

A detailed radiometric model of the system was established to predict the system SNR performance. The model incorporates the at-sensor upwelling radiance, the transmission properties of the optical system, the bandwidth of the individual spectral channels as well as the properties of the detectors and the electronics. The results of the simulation are shown in figure 13 for equivalent 10nm bands (simulation results for individual bands with varying bandwidth are scaled to 10nm bandwidth). The top curve shows the case for the maximum radiance to be measured. For the critical wavelength range around 500nm (ocean sensing) the peak SNR of the instrument is higher than 1000 and at 2200nm the peak SNR is still above 300. The central trace shows the situation for the mission reference observation scenario.

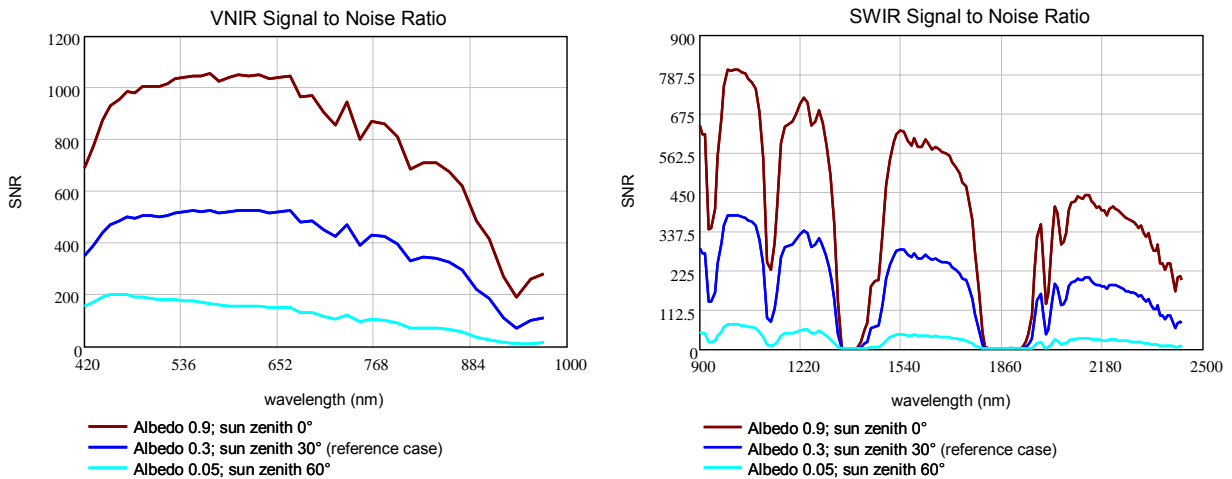


Fig. 13 Predicted SNR performance for the EnMAP Instrument for three nadir looking observation situations for 10nm equivalent bandwidth. The central trace is for the reference case with 30° sun-zenith angle and an albedo of 0.3. The dips in the curves are due to the atmospheric absorption features which reduce the number of signal photon in relation to the detection induced noise.

Further simulations with respect to the system polarization sensitivity involving the properties of the AR and mirror coatings show that the system will meet the 5% requirement for both channels with the SWIR channel sensitivity significantly below this level. Modeling the in orbit MTF shows the system to be dominated by the detector MTF and the along track smear. The values specified in table 1 are achieved with margin for manufacturing the optical elements.

6. THERMAL DESIGN

For consistent data quality it is crucial to consider the thermal design of the instrument for several reasons. Using glass prism elements and NiP coated aluminum mirrors the optical design is not athermal. A finite element analysis of the mirrors shows that for temperatures differing from the manufacturing environment by more than $\pm 1\text{K}$ optically significant distortions of the surfaces for the larger mirrors occur. This is due to the CTE mismatch between the NiP coating and the aluminum structure. The focal shift of the image location induced by the combination of glass and aluminum for this temperature range is less than $20\mu\text{m/K}$ with only a small impact on the MTF. As a consequence the absolute temperature of the instrument in space must be kept within $\pm 1\text{K}$ of the alignment temperature throughout the mission. A second requirement for the thermal design of the instrument is necessary in order to meet the specification with respect to the spectral calibration stability. Because the change in the refractive index of the prisms induces a lateral shift of the image location along the spectral axis of the detectors the temperature of the IOU must be kept stable to $\pm 0.5\text{K}$ between the weekly spectral calibration cycles. Finally, for the offset calibration of the IR background signal in the SWIR, the spectrometer housing must be kept within $\pm 0.2\text{K}$ with respect to the temperature at which the background signal was recorded for offset correction. Since data for offset correction are recorded prior to every data take this stability requirement is related only to the maximum duration of a data take of approx. 2 min.

In order to achieve these thermal requirements the IOU is mounted to the platform inside the ICS using its own thermally isolating suspension. Thus the ICS and the platform act as a first thermal barrier to the space environment. Whenever possible sources of power dissipation and heat input such as the IPU, the ICPU and the baffles of the full aperture diffuser and the telescope are mounted to the ICS. Heat sources which must be mounted to the IOU such as the SWIR cooler and camera electronics transfer their dissipated power directly to external radiators via dedicated thermal links. In addition the IOU features a multi-loop thermal control system. Individual control circuits have been foreseen for the inner part of the entrance baffles, the telescope structure as well as for the spectrometers. With this staggered approach which aims at controlling the radiative input through the entrance apertures the seasonal and orbital thermal variations are kept below 0.3K and the gradients at less 0.05K/min for the relevant parts.

7. INSTRUMENT CALIBRATION

Consistent high precision stable data are essential to extract the scientifically relevant information from the recorded spectra as well as for robust post processing routines. This is crucial in view of the large amounts of hyperspectral data which will be processed by automated post processing chains. To ensure a high standard the EnMAP instrument has several subsystems for on-orbit calibration which employ principles that have proven to be successful in other hyperspectral sensors [7], [8].

For absolute radiometric calibration the sun is used as a source of known spectral irradiation and correct spectral composition. A sun illuminated diffuser placed in front of the telescope reflects radiation entering the sun calibration port into the system aperture. Acting as a diffuse reflectance standard the full entrance pupil is simultaneously illuminated by the diffuser for all field points. Figure 14 illustrates the arrangement. The diffuser panel is mounted on a mechanism which allows it to be rotated in front of the telescope aperture for system calibration. Care is taken to keep residual specular reflections from the diffuser from entering the FOV of the telescope. The baffle design for the sun calibration port is such that stray reflections changing the well defined irradiance situation on the panel are avoided. Spectralon has been selected as diffuser material since it has been demonstrated to be a stable standard of diffuse reflectance in a space environment [9]. In the storage position of the mechanism the diffuser will be sheltered by a protection cover to prevent constant UV exposure causing premature degradation. For conversion to physical units EnMAP will use the new Kurucz solar irradiance spectrum [10] and the measured BRDF of the diffuser panel.

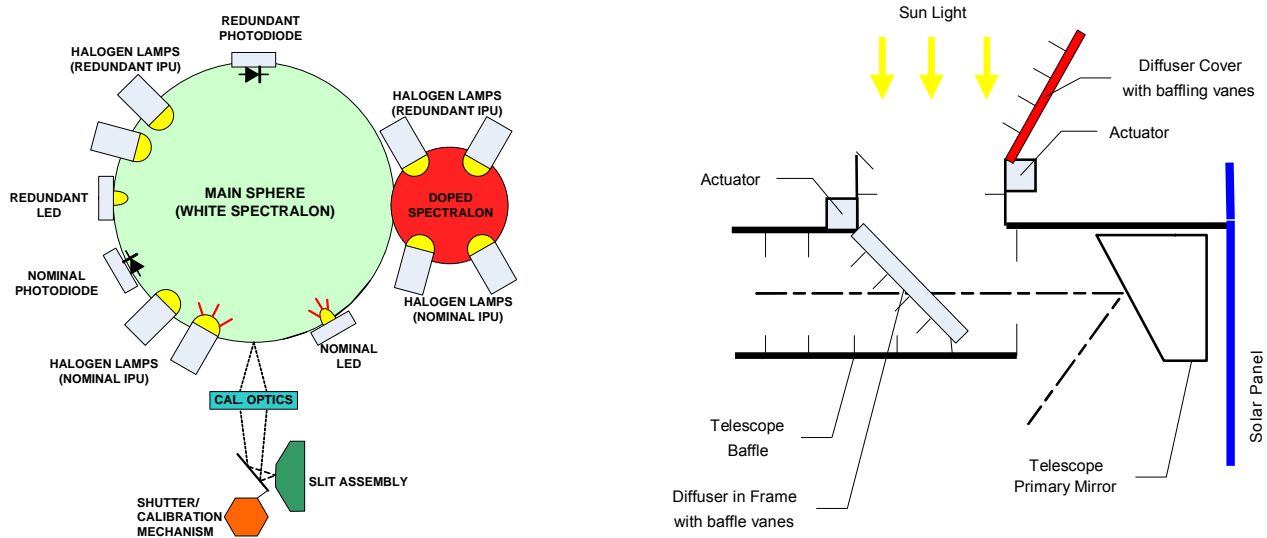


Fig. 14 Onboard calibration units of the EnMAP instrument. For spectral and relative radiometric calibration the Ulbricht sphere (left) provides a homogeneous source of illumination for the spectrometer entrance slits via coupling optics and a mechanism which introduces a mirror into the telescope beam. Absolute radiometric calibration is performed by using the sun to illuminate the entrance pupil of the telescope via a Spectralon full aperture diffuser (right).

For spectral calibration and the determination of the sensor linearity the instrument is equipped with an additional on-board facility. The spectrometer entrance slits will be homogeneously illuminated by the radiation emanating from an integrating sphere. Light from the output port of the sphere is imaged onto the field splitter unit using a dedicated optical system with a mirror mounted to the shutter/calibration mechanism. This mechanism features three positions for observation and absolute radiometric calibration (telescope input), spectral calibration (sphere input) and dark current measurement (shutter). The calibration facility is schematically depicted in figure 14.

The polytetrafluoroethylene sphere is equipped with several light sources and monitoring photodiodes to provide various stable levels of illumination and the spectra for the different calibration tasks. Tungsten halogen lamps driven by precision current sources provide smooth broad spectrum radiation. Due to the spectral mismatch between the solar and the lamp spectra LEDs are added to enhance the short wavelength output of the sphere, an approach which has been demonstrated to be viable for spectrometer calibration in space [11]. For spectral calibration a second smaller sphere couples a light with a strongly structured spectral flux into the primary sphere. Many distinct and stable spectral features are created by combining light from tungsten filament lamps with Erbium doped Spectralon as a diffuser material. All light sources are featured multiple times for redundancy and to monitor degeneration.

8. CONCLUSION

We have presented a mature and robust design for the EnMAP hyperspectral sensor. The instrument uses an innovative spectrometer design together with leading edge technology for the detectors to fulfill the scientific requirements. Due to the thermal stabilization of the optical unit and the availability of on-board calibration facilities to monitor the space environment induced changes of the instrument response the EnMAP data products will feature consistent high quality. The German Space Agency is currently planning to initiate Phase C/D in 2008 with a target launch date for the mission in 2012.

ACKNOWLEDGEMENTS

The work presented in this paper was performed on behalf of the German Space Agency DLR with funds of the German Federal Ministry of Economic Affairs and Technology under the grant No. 50 EP 0601. The authors are responsible for the contents of this publication.

REFERENCES

- [1] Mouroulis P., *Spectral and spatial uniformity in pushbroom imaging spectrometers*, Proc. SPIE 3753, 133-141 (1999).
- [2] Ulbrich, G.J., Meynart R., Nieke J., *APEX-airborne prism experiment: the realization phase of an airborne hyperspectral imager*, Proc. SPIE 5570, 453-459 (2004).
- [3] Féry, Ch., *A prism with curved faces for spectrograph or spectroscope*, Astrophysical Journal 34, 79-87 (1911).
- [4] Wetherell W. and Womble D., *All-Reflective Three Element Objective*, US Patent 4240707 (1980).
- [5] Nieke J., Solbrig M., Neumann A., *Noise contributions for imaging spectrometers*, Appl. Opt. 38(24), 5191-5194 (1999).
- [6] www.aim-ir.de, AIM Infrarot Module GmbH, Theresienstr 2, 74072 Heilbronn, Germany
- [7] Jarecke P.; Yokoyama K.; Barry P., *On-orbit radiometric calibration the Hyperion instrument*, Geoscience and Remote Sensing Symp., IEEE , 6, 2825-2827 (2001).
- [8] European Space Agency, *MERIS Detailed Instrument Description*, Issue 1.0 (2006).
- [9] Bruegge C. et al., *Use of Spectralon as a diffuse reflectance standard for in-flight calibration of earth-looking sensors*, Opt. Eng. 32(4), 805-814 (1993).
- [10] Kurucz, R. L., *The solar irradiance by computation*, in Proc. of the 17th Annual Conference on Atmospheric Transmission Models, G. P. Anderson, R. H. Picard, J. H. Chetwind, eds., 333-334 (1995).
- [11] Nieke J. et al., *Spaceborne Spectrometer Calibration with LEDs*, Proc. SPIE 4135, 384-394 (2000).